AGU PUBLICATIONS

JGR

Journal of Geophysical Research: Earth Surface

RESEARCH ARTICLE

10.1002/2015JF003793

Statistical characterization of spatiotemporal sediment dynamics in the Venice lagoon

Luca Carniello[1], Andrea D'Alpaos[2], Gianluca Botter[1], and Andrea Rinaldo[1,3]

[1]Department of Civil, Environmental and Architectural Engineering (ICEA), University of Padova, Padua, Italy, [2]Department of Geosciences, University of Padova, Padua, Italy, [3]Laboratory of Ecohydrology ECHO/IEE/ENAC, Ècole Polytechnique Fèdèrale de Lausanne, Lausanne, Switzerland

Key Points:
- Wind-wave-induced resuspension events can be modeled as marked Poisson processes
- Interarrival time, intensity, and duration of erosion events are space dependent
- Benthic vegetation strongly affects sediment dynamics

Supporting Information:
- Supporting Information S1

Correspondence to:
Luca Carniello,
luca.carniello@dicea.unipd.it

Citation:
Carniello, L., A. D'Alpaos, G. Botter, and A. Rinaldo (2016), Statistical characterization of spatiotemporal sediment dynamics in the Venice lagoon, *J. Geophys. Res. Earth Surf.*, *121*, 1049–1064, doi:10.1002/2015JF003793.

Received 27 MAR 2015
Accepted 9 APR 2016
Accepted article online 2 MAY 2016
Published online 24 MAY 2016

Abstract Characterizing the dynamics of suspended sediment is crucial when investigating the long-term evolution of tidal landscapes. Here we apply a widely tested mathematical model which describes the dynamics of cohesive and noncohesive sediments, driven by the combined effect of tidal currents and wind waves, using 1 year long time series of observed water levels and wind data from the Venice lagoon. The spatiotemporal evolution of the computed suspended sediment concentration (SSC) is analyzed on the basis of the "peak over threshold" theory. Our analysis suggests that events characterized by high SSC can be modeled as a marked Poisson process over most of the lagoon. The interarrival time between two consecutive over threshold events, the intensity of peak excesses, and the duration are found to be exponentially distributed random variables over most of tidal flats. Our study suggests that intensity and duration of over threshold events are temporally correlated, while almost no correlation exists between interarrival times and both durations and intensities. The benthic vegetation colonizing the central southern part of the Venice lagoon is found to exert a crucial role on sediment dynamics: vegetation locally decreases the frequency of significant resuspension events by affecting spatiotemporal patterns of SSCs also in adjacent areas. Spatial patterns of the mean interarrival of over threshold SSC events are found to be less heterogeneous than the corresponding patterns of mean interarrivals of over threshold bottom shear stress events because of the role of advection/dispersion processes in mixing suspended sediments within the lagoon. Implications for long-term morphodynamic modeling of tidal environments are discussed.

1. Introduction

Resuspension, transport, and deposition of sediments in coastal areas, estuaries, and lagoons play a critical role in many environmental issues such as morphodynamic equilibrium [e.g., *Fagherazzi et al.*, 2006; *D'Alpaos et al.*, 2011; *Mariotti and Fagherazzi*, 2013; *Mariotti and Carr*, 2014], dredging management, transport of pollutants [*Yang and Wang*, 2010], and ecosystem productivity [*Lawson et al.*, 2007; *Carr et al.*, 2010]. Wind waves, in particular, are one of the chief mechanisms that control sediment resuspension in shallow microtidal environments [e.g., *Carniello et al.*, 2005; *Fagherazzi et al.*, 2006; *Green and Coco*, 2007; *Callaghan et al.*, 2010] because wave-induced erosion combined with sediment transport by tidal currents are, in many cases, the leading landforming agents of shallow estuaries and lagoons (see *Green and Coco* [2014] for a review). Recent studies have further suggested that biological processes must be properly accounted for in the study of sediment dynamics for attaining reliable predictions of the morphological evolution of tidal environments [*Folkard*, 2005; *Temmerman et al.*, 2007; *D'Alpaos et al.*, 2007a; *Kirwan and Murray*, 2007; *Moore and Jarvis*, 2008; *Hendriks et al.*, 2010; *Mudd et al.*, 2010; *Marani et al.*, 2010]. For example, the presence of polymeric microphytobenthic biofilm can significantly increase the bottom strength [e.g., *Amos et al.*, 2004], while bioturbation effects linked to crab-halophytic plant interaction may affect the development of tidal creeks [*Perillo et al.*, 2005; *Hughes et al.*, 2009]. Similarly, the presence of benthic vegetation colonizing subtidal platforms, in relation to its specific biophysical characteristics (root apparatus, canopy stiffness, and density), can affect local hydrodynamic properties and increase stability of the bottom sediments [e.g., *Nepf and Vivoni*, 2000; *Venier et al.*, 2012], thereby creating clearer water column and a positive feedback on vegetation growth [e.g., *Carr et al.*, 2010, 2015]. In addition, halophytic vegetation over salt marshes can actively affect landscape evolution by tuning soil elevation within preferential ranges of optimal adaptation [*Marani et al.*, 2013; *Da Lio et al.*, 2013; *D'Alpaos and Marani*, 2015].

Given the complexity of the underlying physical processes, observational evidence represents the most precise and straightforward methodology to address the study of sediment dynamics in tidal environments. Monitoring of suspended sediment concentration (hereafter SSC) is typically based on either in situ point measurements [*Wren et al.*, 2000; *Gartner*, 2004] or satellite image analysis through remote sensing techniques [*Ruhl et al.*, 2001; *Volpe et al.*, 2011]. Satellite-retrieved data provide instantaneous spatially distributed information on the SSC. However, the temporal dynamics of the process can hardly be monitored for several reasons: (i) satellites have a fixed and often long revisit period (e.g., several days); (ii) the most influential resuspension events typically occur during intense storms, which are unfrequent and rarely last more than 1 day; and (iii) storm events are frequently characterized by the presence of clouds, which undermine the analysis of satellite images. As a consequence, multiple satellite acquisitions during single-resuspension events are seldom available, thus preventing the use of this type of data for continuous monitoring of sediment dynamics. On the contrary, in situ point observations (e.g., acoustic or optical backscatter sensors) provide precise information on the temporal dynamics of the local SSC but can hardly provide information about the underlying spatial variability. As a matter of fact, point measurements are usually too sparse compared to the integral scale that defines the heterogeneity of the physical processes involved in sediment resuspension and transport, thereby preventing the use of standard interpolation techniques. Moreover, biofouling may compromise acoustic and optical sensors installed in point turbidity stations, which require periodic cleaning and maintenance. Therefore, reliable long-term SSC records, which are necessary for statistical analyses of the type performed herein, are seldom available.

In order to exploit in situ point observations and satellite images, and overcome their inherent shortcomings, these type of data can be simultaneously incorporated into numerical models [e.g., *Ouillon et al.*, 2004; *Neumeier et al.*, 2008; *Carniello et al.*, 2014] that allow a proper description of the main processes affecting sediment resuspension and transport. After a proper calibration and validation, physically based numerical models can be used to interpolate SCC observations in space and time and thus provide a robust basis for investigating spatial and temporal patterns of suspended sediments in tidal environments.

To this end, a previously tested and calibrated full-fledged Wind Wave-Tidal Model (WWTM) [*Carniello et al.*, 2005, 2011] coupled with a Sediment Transport Model [*Carniello et al.*, 2012] has been applied to the Venice lagoon. The resulting spatial and temporal dynamics of modeled SSC records have been analyzed using the peak over threshold theory, in a framework similar to that used by *D'Alpaos et al.* [2013] for the analysis of the wave-induced bottom shear stresses (BSSs). Our analyses provide a statistically meaningful, spatially explicit characterization of emerging SSC patterns in the Venice lagoon and allow the identification of the links among the major physical processes that control sediment dynamics and the related morphodynamic evolution of shallow tidal basins.

The statistical characterization of resuspension events in space and time bears important implications for long-term modeling of tidal environments. In fact, modeling tidal-landscape morphodynamic evolution over timescales of, say, centuries necessarily requires the use of simplified approaches [e.g., *Murray*, 2007] owing to the computational burden associated to more refined approaches relying on full-fledged numerical models. On the other hand, predicting the long-term evolution of tidal environments [e.g., *Morris et al.*, 2002; *Temmerman et al.*, 2003; *Fagherazzi et al.*, 2006; *D'Alpaos et al.*, 2007a; *Kirwan and Murray*, 2007; *Marani et al.*, 2007; *Mudd et al.*, 2009; *D'Alpaos et al.*, 2011] requires information on sediment supply, which is often assumed as constant. We speculate that the analysis provided in this paper sets a framework to formulate more realistic assumptions on the nature of the sediment supply in simplified models for shallow tidal environments and achieve improved predictions on their long-term morphological evolution.

2. Methods and Data

In the present study we analyze 1 year long records of SSC computed applying a fully coupled Wind Wave-Tidal Model to the Venice lagoon (Figure 1), a worldly famous tidal environment facing the Adriatic sea along the northeastern coast of Italy. The lagoon is a $\approx$550 km^2 wide shallow basin connected to the Adriatic Sea by the three inlets of Lido, Malamocco, and Chioggia and is characterized by an average tidal range of about 1 m, with maximum semidiurnal tidal excursions of $\pm$0.75 m around mean sea level which can suddenly be increased by meteorological forcing. In the following we briefly describe the numerical model highlighting its peculiarities, the 1 year long simulation performed to obtain the SSC time series, and the peak over threshold (POT) method used to analyze the modeled SSC records.

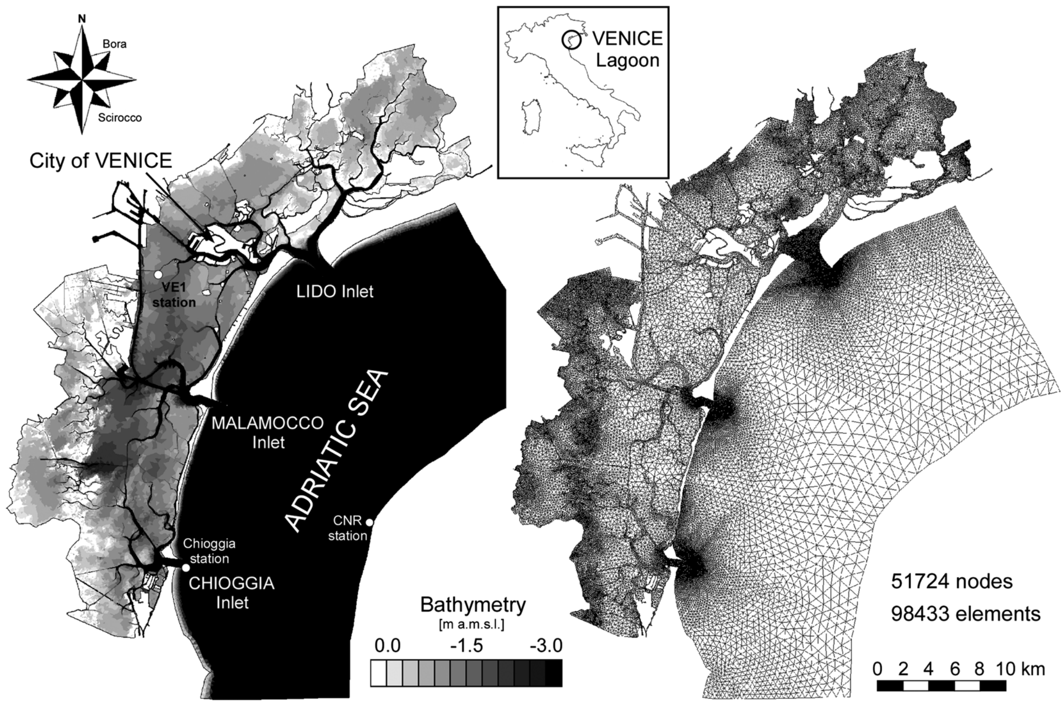

Figure 1. Color coded bathymetry of the Venice lagoon and computational grid used for the numerical simulations. The locations of the stations where boundary conditions (Chioggia and CNR-station) are collected and where numerical results are locally analyzed (VE1 station) are also shown.

2.1. Numerical Model

The numerical model consists of three modules: the hydrodynamic module coupled with the wind-wave module (WWTM) [*Carniello et al.*, 2005, 2011] and the sediment transport and bed evolution module (STABEM) [*Carniello et al.*, 2012], which describes the relevant morphodynamic processes.

The *hydrodynamic module* solves the 2-D shallow water equations suitably modified in order to reproduce flooding and drying processes in very shallow and irregular domains. The governing equations are solved using a semiimplicit staggered finite element method based on Galerkin's approach (see *Defina* [2000], *Martini et al.* [2004], and *D'Alpaos and Defina* [2007] for a detailed description of the equations and of the numerical scheme). Considering the case of a turbulent flow over a rough wall, the bottom shear stress induced by tidal currents, τ_{tc}, is evaluated using the Strickler formula. The hydrodynamic module provides the wind-wave module with the flow field characteristics necessary to describe the processes affecting wind-wave generation and propagation.

The *wind-wave module* [*Carniello et al.*, 2011] is based on the solution of the wave action conservation equation parameterized using the zero-order moment of the wave action spectrum in the frequency domain. The spatial and temporal distribution of the wave period is determined through an empirical correlation function relating the peak wave period to the local wind speed and water depth [*Young and Verhagen*, 1996; *Breugem and Holthuijsen*, 2006; *Carniello et al.*, 2011]. The bottom shear stress induced by wind waves, τ_{ww}, is computed in the wind-wave module as a function of the maximum horizontal orbital velocity at the bottom, which is related to the significant wave height through the linear theory. Because of the nonlinear interaction between the wave and current boundary layers, the maximum bottom shear stress, τ_{wc}, resulting from the combined effect of tidal currents and wind waves is enhanced beyond the sum of the two contributions, as accounted for in the WWTM on the basis of the empirical formulation suggested by *Soulsby* [1997]. It is worthwhile pointing out that the WWTM has been widely tested by comparing model results to hydrodynamic and wind-wave data collected not only in the Venice lagoon [*Carniello et al.*, 2005; *D'Alpaos and Defina*, 2007; *Carniello et al.*, 2011] but also in the lagoons of the Virginia Coast Reserve, USA [*Mariotti et al.*, 2010].

The *sediment transport and bed evolution module* (STABEM) solves the advection diffusion equation and the Exner's equation considering the same computational gird of WWTM.

In order to consider the simultaneous presence of cohesive and noncohesive sediment typically characterizing tidal lagoons, STABEM uses two size classes of sediments to describe the bed composition: noncohesive sand and cohesive mud (sum of clay and silt) [*Van Ledden et al.*, 2004]. The transition between noncohesive and cohesive behavior of the mixture and the critical value for the bottom shear stress are determined as a function of the updated local mud content (which varies both in space and time) on the basis of the critical value assumed for pure sand and pure mud. The use of a sediment mixture requires a reliable reconstruction of the initial configuration of the bed composition, which is a difficult and site-specific task. Available field data are, in most cases, limited as compared to the spatial variability of bed composition, thus preventing the use of purely statistical approaches. To overcame this problem, field survey in the Venice lagoon have been carried out, which allowed the identification of an empirical relationship between the local bed composition and both the local bottom elevation and the distance from the nearest inlet. This relationship has been used to reconstruct a reliable initial bed composition (see Figure S1 in the supporting information).

Another peculiar feature of the sediment transport module is the stochastic approach (similar to that suggested by *Grass* [1970]) adopted to reproduce the near-threshold conditions for sediment entrainment, which usually characterize shallow tidal basins where resuspension events occur periodically driven by bottom shear stresses that slightly exceed the erosion threshold. Both the total bottom shear stress (induced by the combined effect of waves and currents) and the critical shear stress for erosion are treated as random variables (τ'_{wc} and τ'_c, respectively) with lognormal probability distributions. The space- and time-varying values of the total bottom shear stress, τ_{wc}, and of the critical shear stress, τ_c, computed by STABEM represent the expected values of the two distributions. Following the stochastic approach, the erosion rate is assumed to depend on the probability that τ'_{cw} exceeds τ'_c which is calculated accounting for the randomness of τ_{wc} and τ_c. Figure S2 in the supporting information shows the comparison between the transport parameter, T (which governs the entrainment flux), computed using the classic deterministic formulation, $T = \max(0; \tau_{wc}/\tau_c - 1)$ [*Van Rijn*, 1984], and the stochastic approach [*Carniello et al.*, 2012]. In the same figure we show the comparison between the SSC computed considering both the deterministic formulation for T and the stochastic approach, as well as the SSC data collected at one station located in the central-southern part of the lagoon during a quite intense storm event characterized by Bora wind (blowing from NE) which is a typical storm condition for the Venice lagoon. The plot suggests that the deterministic formulation for T is not able to correctly predict the time evolution of the local turbidity especially for the lower SSC values and at near-threshold conditions. Instead, the stochastic approach allows for an improved agreement with observed data. Figure S2 in the supporting information further shows that during storm events, the SSC can exceed 200 mg/L in the fetch unlimited central part of the lagoon. For a complete description of STABEM and further comparisons with actual data from the Venice lagoon the reader is referred to *Carniello et al.* [2012].

The comparison with SSC retrievals from remote sensing data further enabled us to assess the ability of the model to properly describe observed spatial patterns of SSC [*Carniello et al.*, 2014]. These studies highlighted, in particular, the crucial role exerted by the sheltering effect associated to artificial structures and natural intertidal landforms on SSC patterns and clearly showed the stabilizing effect of benthic vegetation that highly affects sediment dynamics at the system scale.

2.2. Numerical Simulations

The numerical model presented in section 2.1 was used to perform a 1 year long simulation within a computational grid that reproduces the Venice lagoon and a portion of the Adriatic Sea (see Figure 1). Boundary conditions and forcing terms are the time records of tidal levels and wind velocity and directions observed during the whole year 2005 in the Venice lagoon. In particular, we used hourly tidal levels measured at the Consiglio Nazionale delle Ricerche (CNR) Oceanographic Platform, located in the Adriatic Sea in front of the Venice lagoon, as well as wind velocities and directions observed at the Chioggia anemometric station (see Figure S3 in the supporting information), for which a quite long historical record of wind data is available. The year 2005 was selected as “representative” of the typical behavior of wind fields in the Venice lagoon [*D’Alpaos et al.*, 2013] because the probability distribution of wind velocities during 2005 was shown to be the closest to the average distribution observed between 2000 and 2008.

As previously mentioned, an issue that needs be considered when modeling the spatial variability of SSC is the presence of benthic and halophytic vegetation, which both shelters the bed against the action of current-induced and wave-induced bottom shear stress and increases the local critical shear stress for erosion because of the presence of roots. While the presence of halophytic vegetation over the salt marshes

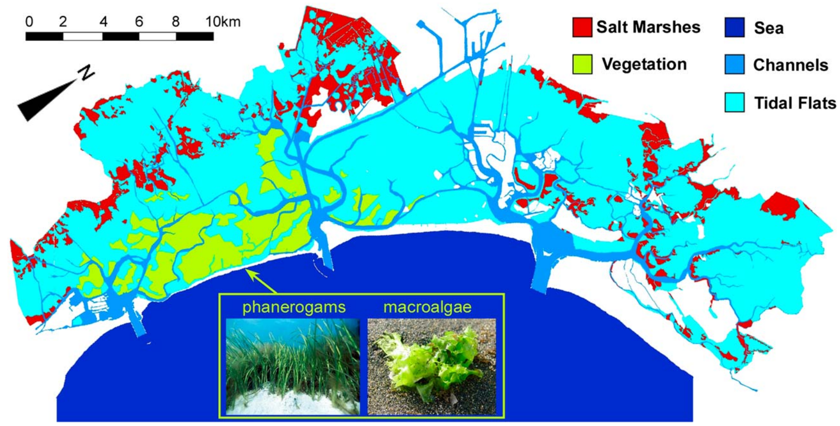

Figure 2. Spatial distribution of the main morphological features characterizing the Venice lagoon. The light green areas represent the maximum extent of the sea grass meadow (phanerogams and macroalgae) derived on the basis of the monitoring activities carried out by the Venice Water Authority in 2002, 2003, and 2004 [*SELC*, 2005].

(e.g., *Spartina maritima*, *Limonium narbonense*, *Salicornia veneta*, and *Sarcocornia fruticosa*) can be easily detected, mapping the presence of benthic vegetation that colonizes tidal flats and subtidal platforms is more difficult. In the specific case of the Venice lagoon, only subtidal platforms located in central southern part of the basin are populated by well-established sea grass meadows characterized by the simultaneous presence of phanerogams (*Zostera marina* and *Cymodocea nodosa*) and macroalgae (*Ulva rigida*). A proper quantification of the stabilizing effect of benthic vegetation at the scale of the entire lagoon is a difficult task. First of all, different vegetation species affect in different ways both local hydrodynamics and bed strength [e.g., *Nepf and Vivoni*, 2000; *Lopez and Garcia*, 2001; *Venier et al.*, 2012]. Moreover, their spatial distribution may be extremely variable in response to seasonal variations and vegetation-sediment-water flow interactions [e.g., *Curiel et al.*, 2004; *Carr et al.*, 2010; *Hendriks et al.*, 2010].

For the above reasons the stabilizing effect of vegetation was modeled in STABEM by setting to zero the sediment resuspension flux in the areas of the computational domain colonized by vegetation, regardless of the species involved [*Carniello et al.*, 2014]. In our analyses, salt marshes were all assumed to be colonized by halophytic vegetation while the extent of the sea grass meadows was assumed equal to the maximum extent of the vegetation coverage determined on the basis of field surveys carried out by the Venice Water Authority from 2002 to 2004 [*SELC*, 2005] (see Figure 2). Needless to say, more accurate parametrization could be developed that exploit detailed data on the spatiotemporal evolution of vegetation coverage, including, e.g., in situ observation and information derived from satellite images. In order to highlight the importance of the biostabilizing effect of benthic vegetation two different simulations were preformed, both neglecting and accounting for the presence of the sea grass meadows within the lagoon. Such an approach aims at exploring the maximum stabilization potential associated with submerged vegetation and allows one to obtain an objective assessment of the effect of biostabilizing processes on sediment resuspension in tidal environments.

2.3. Peak Over Threshold Analysis

Sediment transport dynamics in tidal environments are the byproduct of complex hydrodynamic, biologic and geomorphologic processes that include both deterministic and stochastic components. In particular, it has been argued that the morphological evolution of the Venice lagoon is mostly related to a limited number of intense resuspension events induced by wind waves [*Carniello et al.*, 2011], whose dynamics are markedly stochastic [*D'Alpaos et al.*, 2013; *Venier et al.*, 2014]. Here the spatiotemporal patterns of morphologically meaningful resuspension events in the Venice lagoon are analyzed using the theory of the peak over threshold (POT) [*Balkema and de Haan*, 1974]. First, a set of events is identified and selected from the modeled record of SSCs by means of a minimum-intensity threshold (C_0). A statistical analysis of the interarrivals, durations, and intensities of the exceedances of the selected threshold is then carried out. The interarrival time (T) is defined as the time elapsed between two consecutive upcrossing of the threshold, while the duration (D) of the events is the time elapsed between any upcrossing and the subsequent downcrossing of the threshold. Finally, the intensity (E) is calculated as difference between the maximum value of SSC in the time lapse between the upcrossing and the downcrossing, and the threshold C_0. These variables are described by means of their probability density functions and the corresponding moments. The analysis is performed pointwise and repeated for all the locations of the Venice lagoon so as to provide an accurate description of the spatiotemporal patterns of SSC.

While the adopted methodology resembles that used by *D'Alpaos et al.* [2013] to characterize the patterns of bottom shear stresses, in this paper the statistical analysis is extended to the dynamics of suspended sediments, with particular emphasis on the role of morphological and vegetation features.

The distribution of the interarrivals plays a pivotal role in characterizing the nature of stochastic point processes. In our case, if the interarrival times between subsequent exceedances of C_0 are independent and exponentially distributed random variables, SSC dynamics can be mathematically described as a marked Poisson process, where a vector of random marks (intensity and duration of each over threshold event) is associated to a sequence of random events that define a 1-D Poisson process along the time axis. Poisson processes are characterized by mathematical features such as the memoryless property, owing to which the number of events observed in disjoint subperiods are independent, Poisson-distributed random variables. The extreme value theory postulates that stochastic signals allow for the general emergence of Poisson processes whenever the censoring threshold is high enough [*Cramer and Leadbetter*, 1967]. However, as we shall note in the following, in the present analysis the threshold is maintained well below the maximum observed values, as it is designed to remove only the confounding effect of weak resuspension events induced by tidal currents. Hence, the proposed analysis is likely to apply not only for the description of the extreme events but also for the characterization of the bulk effect of morphologically meaningful resuspension events. The theoretical and computational advantages implied by Poisson processes are manifold and include the ease of computation and the suitability to analytical manipulations. In fact, the Poissonianity of resuspension events would allow one to retain all the sources of stochasticity in the physical drivers of sediment mobilization (e.g., wind, waves, and critical shear stress) into a single parameter (the mean frequency of the process λ) which, in turn, can be used to calculate the average number of resuspension events ($\langle n \rangle$) taking place during any reference period of duration ΔT as $\langle n \rangle = \lambda \Delta T$. Hence, the integrated effect of time-varying forcings can be easily accounted for via Monte Carlo realizations of sequences of events or through analytical techniques that allow the problem to be cast in probabilistic terms, providing insight on the emergent long-term behavior of the system.

While the use of Poisson processes for the analytical characterization of the long-term behavior of geophysical processes driven by stochastic agents is becoming increasingly popular in hydrology and geomorphology [e.g., *Rodriguez-Iturbe et al.*, 1987; *D'Odorico and Fagherazzi*, 2003; *Botter et al.*, 2007, 2013; *Park et al.*, 2014], applications to tidal environments are still relatively rare [*D'Alpaos et al.*, 2013] and represent a promising framework.

3. Results and Discussion

First, the results of the simulation performed were analyzed by neglecting the stabilizing effect of the sea grass meadows colonizing the central southern part of the lagoon. The numerical results provide, at each location within the Venice lagoon, the temporal evolution of the SSC which can be analyzed on the basis of the POT theory in order to assess whether resuspension events can be represented as a Poisson process. To test quantitatively the latter assumption, we performed a Kolmogorov-Smirnov (KS) goodness of fit test at significance level $\alpha = 0.05$. Following the approach suggested by *D'Alpaos et al.* [2013], the time series of SSCs were preliminarily low-pass filtered through a moving average operation in order to remove short-term fluctuations leading to spurious upcrossing and downcrossing of the prescribed threshold, which would have artificially affected the correlation between subsequent over threshold events. A 6 h moving time window was adopted for the low-pass filtering in order to preserve the signal modulation induced by semidiurnal tidal oscillations.

A set of preliminary analyses was performed to assess the impact of the choice of the threshold value (C_0) that identifies the morphologically meaningful resuspension events in our analyses. On the one hand, C_0 must be large enough to separate stochastic resuspension events driven by storm-induced wind waves from daily concentration dynamics modulated by tidal currents. On the other hand, C_0 should not be too high in order to avoid significant loss of information (as all the events smaller than C_0 are neglected) and retain the bulk effect of resuspension processes.

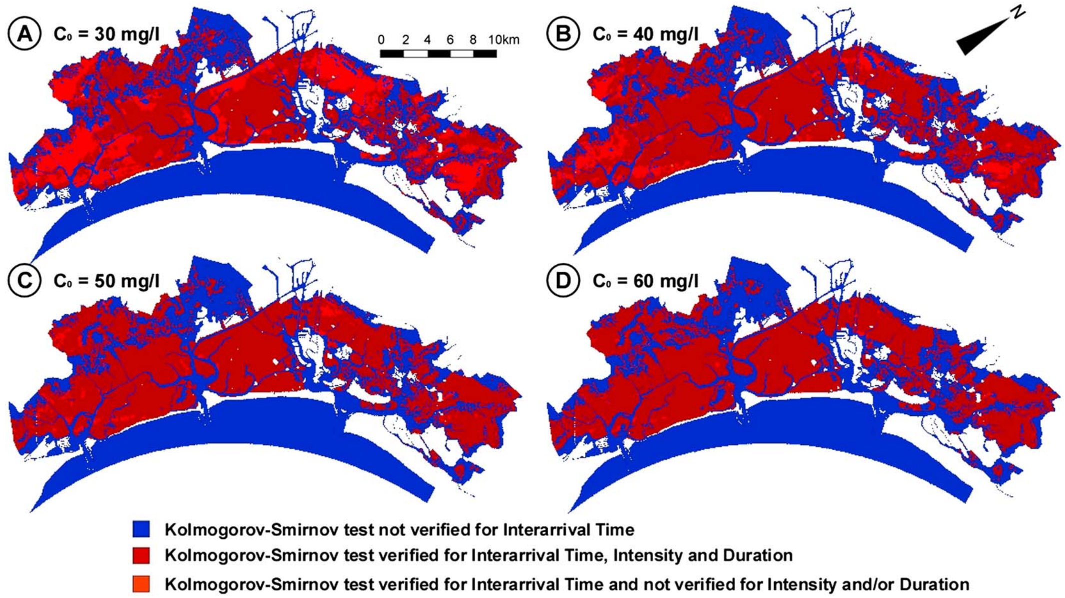

Figure 3. Maps providing the spatial distribution of the Kolmogorov-Smirnov (KS) test at significance level $\alpha = 0.05$ for different threshold values, C_0, of the SSC: (a) 30 mg/L; (b) 40 mg/L; (c) 50 mg/L; (d) 60 mg/L. In the maps we distinguish areas where the KS test is: not verified (blue); verified for all the considered stochastic variables (interarrival time, intensity over the threshold, and duration) (red); verified for the interarrival time and not for intensity and/or duration (orange).

Figure 3 shows the spatial distribution of the outcome of the Kolmogorov-Smirnov (KS) test within the Venice lagoon considering four different C_0 values in the range 30–60 mg/L. The four maps of Figure 3 show the areas where the KS test is: (i) not verified for the interarrival time (blue areas)—i.e., resuspension events cannot be described as a Poisson process; (ii) verified for all the three stochastic variables considered, namely interarrival times, intensity, and duration (red areas)—i.e., resuspension events are indeed a marked Poisson process where also intensity and duration are exponentially distributed random variables; and (iii) verified for the interarrival time but not for intensity and/or duration (orange areas)—i.e., resuspension events are a

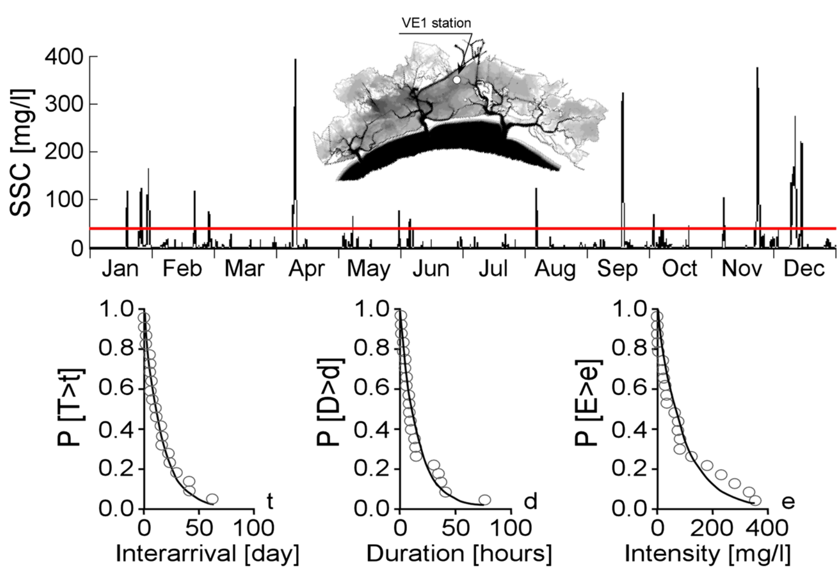

Figure 4. (top) Time series of the computed SSC at the VE1 station (see map for the location) resulting from the combined effect of tidal currents and wind waves. (bottom row) The probability distributions of interarrival times, intensities of peak excesses in the SSC over the threshold $C_0 = 40$ mg/L (i.e., maximum intensities of the exceedances during an event, E = $(C - C_0)_{max}$), and durations of over threshold events. The circles represent the computed probability distributions, while the solid lines represent the theoretical exponential trend.

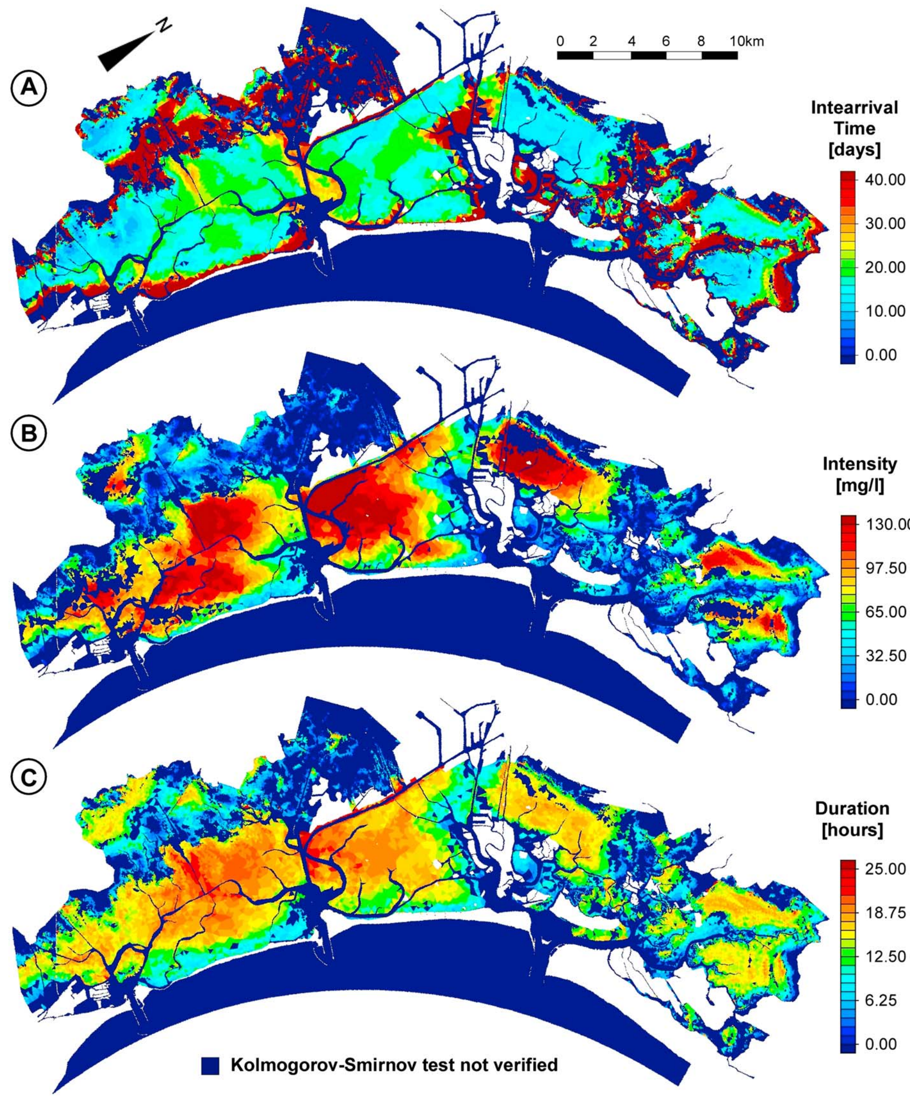

Figure 5. Spatial distributions of (a) mean interarrival times, (b) mean intensities of peak excesses, and (c) mean durations of over threshold exceedances. Dark blue identifies sites where resuspension events cannot be modeled as a marked Poisson process (i.e., the KS test is not verified for the interarrival times).

marked Poisson process but at least one between intensity and duration is not an exponentially distributed random variable. Figure 3 shows that the portions of the lagoon where resuspension events cannot be modeled as a marked Poisson process are mostly represented by salt marshes and tidal channels. In particular, no exceedances of the threshold C_0 occur over the salt marshes because the reduced water depth and the presence of halophytic vegetation limit the wave height and stabilize the bottom [e.g., *Carniello et al.*, 2005; *Möller et al.*, 1999]. On the contrary, at the three inlets and within the main tidal channels, exceedances of the threshold are observed, but these are mostly related to peak excesses promoted by tidal currents, which are deterministic processes and thus cannot be modeled as random Poisson processes. Interestingly, the extent of the areas where the KS test is verified is weakly affected by changes in the threshold value. Hence, a constant threshold $C_0 = 40$ mg/L was used in the following analysis.

As an example Figure 4 provides the time evolution of the SSC at the VE1 station located in a subtidal platform (depth of about 1.5 m below MSL) in the central part of the lagoon (see also Figure 1). The three plots in the lower part of Figure 4 compare the computed (circles) exceedance probability of interarrival times, maximum intensities, and durations of the over threshold events with the theoretical exponential trends (solid lines). We first observe that the interarrival time of resuspension events is well described by an exponential distribution as confirmed also by the results of the KS test, which is indeed satisfied at significance level $\alpha = 0.05$.

Table 1. Spatially Averaged Value of Mean Interarrival Time, $1/\tilde{\lambda}_{C,t}$, Mean Intensity, $1/\tilde{\lambda}_{C,e}$, and Mean Duration, $1/\tilde{\lambda}_{C,d}$ [a]

Spatially Averaged	No Benthic Vegetation	With Benthic Vegetation
$1/\tilde{\lambda}_{C,t}$ (days)	29.24	36.17
$1/\tilde{\lambda}_{C,e}$ (mg/L)	73.21	66.72
$1/\tilde{\lambda}_{C,d}$ (h)	13.96	13.86
$\tilde{CV}_{C,t}$	1.103	1.034
$\tilde{CV}_{C,e}$	0.545	0.563
$\tilde{CV}_{C,d}$	0.336	0.345
$\tilde{\rho}_{C,te}$	−0.467	−0.454
$\tilde{\rho}_{C,td}$	−0.490	−0.425
$\tilde{\rho}_{C,ed}$	0.831	0.795

[a]Coefficient of variation of mean interarrival time, $\tilde{CV}_{C,t}$; mean intensity, $\tilde{CV}_{C,e}$, and mean duration, $\tilde{CV}_{C,d}$. Spatial cross correlation of mean interarrival time and mean intensity, $\tilde{\rho}_{C,te}$, mean interarrival time and mean duration, $\tilde{\rho}_{C,td}$, and mean intensity and mean duration, $\tilde{\rho}_{C,ed}$. Results refer to the analysis of SSC signals (Figure 5) and are provided both neglecting and considering the stabilizing effect of submerged benthic vegetation.

The parameter $\lambda_{C,t}$ of the exponential distribution (fitted using the method of moments) is the mean rate of occurrence of the over threshold events. In the station VE1, this corresponds to a mean interarrival time $1/\bar{\lambda}_{C,t}$ of about 15.7 days. We further note that the results of the KS test suggest that at the VE1 station, also the excess, $E=(C_{\max}-C_0)$, and the duration of the over threshold events are exponentially distributed random variables with mean intensity $1/\bar{\lambda}_{C,e}=98.3$ mg/L and mean duration $1/\bar{\lambda}_{C,d}=16.4$ h.

The analysis is then extended to the entire lagoon. Figure 5 shows the spatial distributions of the mean interarrival times (Figure 5a), mean intensities of peak excesses (Figure 5b), and mean durations (Figure 5c) at any location within the Venice Lagoon in which resuspension dynamics are Poissonian (i.e., the KS test for the interarrival times is satisfied at significance level $\alpha=0.05$).

It is worthwhile recalling that the SSC at any single location depends on the combination of local entrainment and advection/dispersion processes from and toward the adjacent areas. Furthermore, the local entrainment, induced by wind waves and tidal currents, is highly affected by current speed, water depth, wind speed, and fetch. These instances explain the complex and heterogeneous spatial pattern for SSC dynamics represented in Figure 5.

Large interarrival times and small intensities and durations characterize sheltered areas located leeward of spits, marshes, islands, or artificial structures. The presence of natural or artificial barriers is particularly important when considering resuspension events induced by Bora wind, which is the most intense and morphologically significant wind in the Venice lagoon blowing from northeast at speeds which easily exceed 20 m/s. This is highlighted by the innermost areas sheltered by marshes and mainland in the northeastern part of the lagoon, in its western portions and the area located south of the city of Venice (Figure 5). On the contrary, short interarrival times and large intensities and durations, which imply more intense and frequent resuspensions, are observed in the central and southern part of the lagoon, as well as in the area located between the city of Venice and the Marco Polo International airport (Figure 1). Those are indeed the deepest and almost fetch-unlimited subtidal platforms of the lagoon, where wind-wave erosion is more effective [e.g., *Fagherazzi et al.*, 2006; *Defina et al.*, 2007; *D'Alpaos et al.*, 2013] as confirmed by the established erosive trend that those areas have been experiencing since the beginning of the last century [e.g., *Carniello et al.*, 2009; *Molinaroli et al.*, 2009; *D'Alpaos*, 2010]. The spatially averaged values for the mean rate of occurrence of the over threshold events, mean intensity, and mean duration are listed in Table 1 and are about 29 days, 73 mg/L, and 14 h, respectively. If we consider that the surface of tidal flats and subtidal platforms in the Venice lagoon is about 400 km^2 (i.e., excluding fisheries, channels, and salt marshes) and we assume an average water depth of 1.0 m, this means that every month, for 14 h, about 9600 tons of sediments are mobilized within the basin.

In order to provide a quantitative estimation of the spatial heterogeneity of SSC patterns, the spatially averaged coefficients of variation (see supporting information for the mathematical definition) for mean

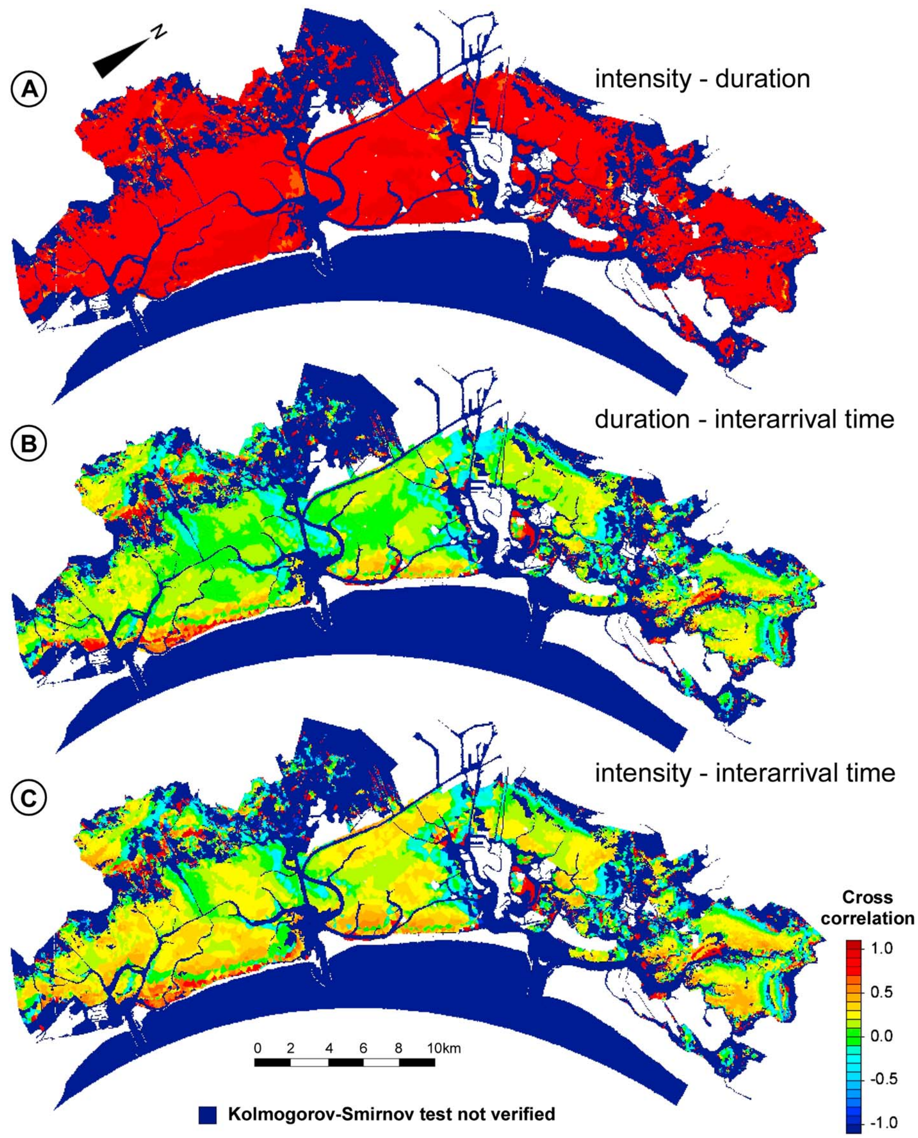

Figure 6. Spatial distributions of temporal cross correlations between (a) intensity of peak excesses and duration of over threshold exceedance, (b) duration and interarrival time, and (c) intensity and interarrival time. Dark blue identifies sites where resuspension events cannot be modeled as a marked Poisson process (i.e., the KS test is not verified for the interarrival time).

interarrival times, $\tilde{CV}_{C,t}$, mean intensities, $\tilde{CV}_{C,e}$, and mean durations, $\tilde{CV}_{C,d}$, have been computed (Table 1). Data show that $\tilde{CV}_{C,t} > \tilde{CV}_{C,e} > \tilde{CV}_{C,d}$, suggesting that the highly irregular morphology characterizing the Venice lagoon mainly affects the spatial distribution of the mean interarrival times of resuspension events. Meanwhile, the spatial distribution of mean intensities and durations is more homogeneous within the computational domain.

Figure 6 shows the temporal cross correlation between the three random variables ($\bar{\rho}_{t,te}$, $\bar{\rho}_{t,td}$, $\bar{\rho}_{t,ed}$—see supporting information for the mathematical definition) computed for each point within the lagoon. The plot indicates that the intensity of peak excesses and duration of over threshold exceedances (Figure 6a) are highly correlated, owing to the pseudo-deterministic link between peak intensities and the corresponding recession dynamics. Conversely, almost no correlation exists between durations and interarrival times (Figure 6b), as well as between intensities and interarrival times (Figure 6c), suggesting that resuspension events can be modeled as a 3-D Poisson process in which the marks (duration and intensity of events) are mutually dependent but independent on the arrival times. We further computed (see Table 1 and supporting information for the mathematical definition) the spatial cross correlation between mean

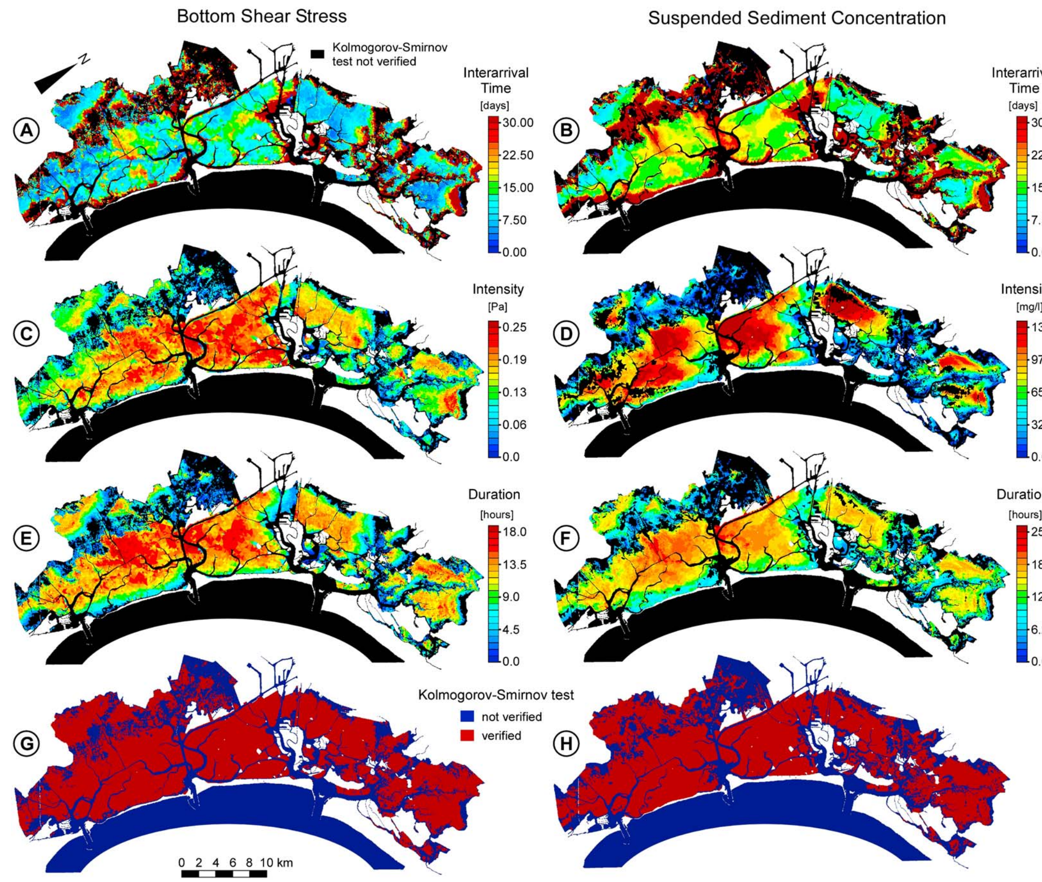

Figure 7. (a, b) Comparison between the spatial distributions of mean interarrival times, (c, d) mean intensities of peak excesses, and (e, f) mean durations of over threshold exceedances obtained analyzing numerical results in term of (Figures 7a, 7c, and 7e) total bottom shear stress and (Figures 7b, 7d, and 7f) suspended sediment concentration. Figures 7a, 7c, and 7e are adapted from *D'Alpaos et al.* [2013].

interarrival times and mean intensities ($\tilde{\rho}_{C,te}$), mean interarrival times and mean durations ($\tilde{\rho}_{C,td}$), and mean intensities and mean durations ($\tilde{\rho}_{C,ed}$). Our analysis confirms that mean intensities and durations are characterized by similar spatial patterns ($\tilde{\rho}_{C,ed} \cong 0.8$). On the contrary the negative values of $\tilde{\rho}_{C,te}$ and $\tilde{\rho}_{C,td}$ indicate that where resuspension events are more frequent (i.e., shorter interarrival time), intensities of peak excesses and durations of exceedances are larger.

In Figure 7 we provide a comparison between the statistical properties of SSC and those of bottom shear stress (BSS). The latter has been calculated accounting for the combined action of currents and waves and by assuming $\tau_c = 0.4$ Pa as threshold value for the POT analysis, as discussed by *D'Alpaos et al.* [2013]. The KS test for the exponentiality of interarrivals is verified in wide portions of the lagoon both for BSS and SSC (Figures 7g and 7h), which means that resuspension events can be modeled as marked Poisson processes both in terms of cause (BSS producing sediment entrainment) and effect (SSC). It is also interesting to observe that the spatial distributions of the mean interarrival time (Figures 7a and 7b), mean peak intensity (Figures 7c and 7d), and mean duration (Figures 7e and 7f) are similar but not identical, which confirms that the two quantities are related by a cause (BSS) and effect (SSC) relationship but they are not equivalent. While the BSS is a function of the local forcings (currents and wind waves) the SSC at any single location depends not only on the local entrainment (i.e., local BSS) but also on the flux of suspended sediment from and toward the surrounding areas. The differences in the spatial patterns of the mean interarrival time, mean peak intensity, and mean duration shown in Figure 7 considering BSSs and SSCs confirm the crucial role of advection/dispersion processes in smoothing the spatial patterns of SSC in the Venice lagoon.

In order to perform a more quantitative comparison between SSC and BSS dynamics, the BSS signal has been used to calculate the spatially averaged value of the mean interarrival time, mean peak excess, and mean

Table 2. Spatially Averaged Values of Mean Interarrival Times, $1/\tilde{\lambda}_{\tau,t}$, Mean Intensities, $1/\tilde{\lambda}_{\tau,e}$, and Mean Durations, $1/\tilde{\lambda}_{\tau,d}$ [a]

Spatially Averaged	No Vegetation
$1/\tilde{\lambda}_{\tau,t}$ (days)	26.18
$1/\tilde{\lambda}_{\tau,e}$ (Pa)	0.146
$1/\tilde{\lambda}_{\tau,d}$ (h)	10.44
$\tilde{CV}_{\tau,t}$	1.479
$\tilde{CV}_{\tau,e}$	0.379
$\tilde{CV}_{\tau,d}$	0.419
$\tilde{\rho}_{\tau,te}$	−0.447
$\tilde{\rho}_{\tau,td}$	−0.445
$\tilde{\rho}_{\tau,ed}$	0.828

[a]Coefficient of variation of mean interarrival times, $\tilde{CV}_{\tau,t}$, mean intensities, $\tilde{CV}_{\tau,e}$, and mean durations, $\tilde{CV}_{\tau,d}$. Spatial cross correlation between mean interarrival times and mean intensities, $\tilde{\rho}_{\tau,te}$, mean interarrival times and mean durations, $\tilde{\rho}_{\tau,td}$, and mean intensities and mean durations, $\tilde{\rho}_{\tau,ed}$. Results refer to the analysis of BSS signals (Figures 7a, 7c, and 7e).

duration, as well as their spatial cross-correlation and the coefficients of variation (see Table 2 and the auxiliary material for the mathematical definition). The comparison with the analogous parameters obtained for the SSC, which are summarized in Table 1 (neglecting the effect of benthic vegetation), suggests that the same considerations done for the SSC also apply to the case of the BSSs. Interestingly, the fact that $1/\tilde{\lambda}_{C,t} \cong 1/\tilde{\lambda}_{\tau,t}$ confirms that the choice of the thresholds adopted for the POT analyses of SCC and BSS signals are consistent. Moreover $\tilde{CV}_{\tau,t} > \tilde{CV}_{C,t}$, which testifies a more heterogeneous spatial distribution of mean interarrival times when considering the BSS instead of the SSC. This confirms the key role of advection/dispersion processes in the observed spatial patterns of SCC, resulting in a notable smoothing of the heterogeneities of local properties like BSS.

Table 3 further provides the average spatial cross correlation between mean interarrival times (Figures 7a and 7b), mean intensities (Figures 7c and 7d), and mean durations (Figures 7e and 7f) computed for both BSSs and SSCs (see supporting information for the mathematical definition). Results show that the most spatially correlated among the three random variables are the mean durations while the mean interarrival times are less correlated.

We finally extended our analysis including in the simulation the biostabilizing effect of benthic vegetation that colonizes the central southern part of the lagoon. Figure 8 provides the planimetric distribution of the difference between the mean interarrival times (Figure 8a), mean intensities of peak excesses (Figure 8b), and mean durations of over threshold exceedances of SCC (Figure 8c) that are computed both neglecting and considering the stabilizing effect of submerged benthic vegetation. As expected, the presence of vegetation significantly affects SSC dynamics by increasing the mean interarrival time of over threshold exceedances (blue colors in Figure 8a). However, the concentration in suspension is exclusively related not only to local entrainment but also to dispersive and advective fluxes from and toward the surrounding areas. Hence, close to the edges of the sea grass meadows, the stabilizing effect of vegetation tends to vanish due to the incoming of suspended sediment conveyed from the neighboring areas. On the other hand, the stabilizing effect tends to expand from the areas colonized by sea grass meadows to the surrounding regions owing to a sheltering effect like the one provided by islands or salt marshes. Needless to say, the size of sea grass meadows is a key issue, as sparse vegetated areas produce limited effects on resuspension and SSC patterns. Compared to the effect of vegetation on the mean interarrival time of significant resuspension events, the effect of vegetation on the spatial distribution of mean intensity and duration is more nuanced (Figures 8b and 8c). Overall, the presence of vegetation reduces both intensity and duration of over threshold events (yellow to red colors in Figures 8b and 8c). However, some areas (e.g., close to the Malamocco inlet) display an increase in both the parameters (green to blue colors in Figures 8b and 8c). This can be ascribed to the fact that owing to the stabilizing effect of vegetation, in such areas only the largest resuspension events enable the exceedance of the threshold when the effect of benthic vegetation is accounted for, thereby leading to increased mean duration and intensity of resuspension events. The analysis of the spatial

Table 3. Spatially Averaged Spatial Cross Correlation Between Mean Interarrival Time for BSS and SSC, Mean Intensities for BSS and SSC, and Mean Durations for BSS and SSC

Cross-Correlation BSS-SSC	No Vegetation
Interarrival time	0.412
Intensity	0.662
Duration	0.802

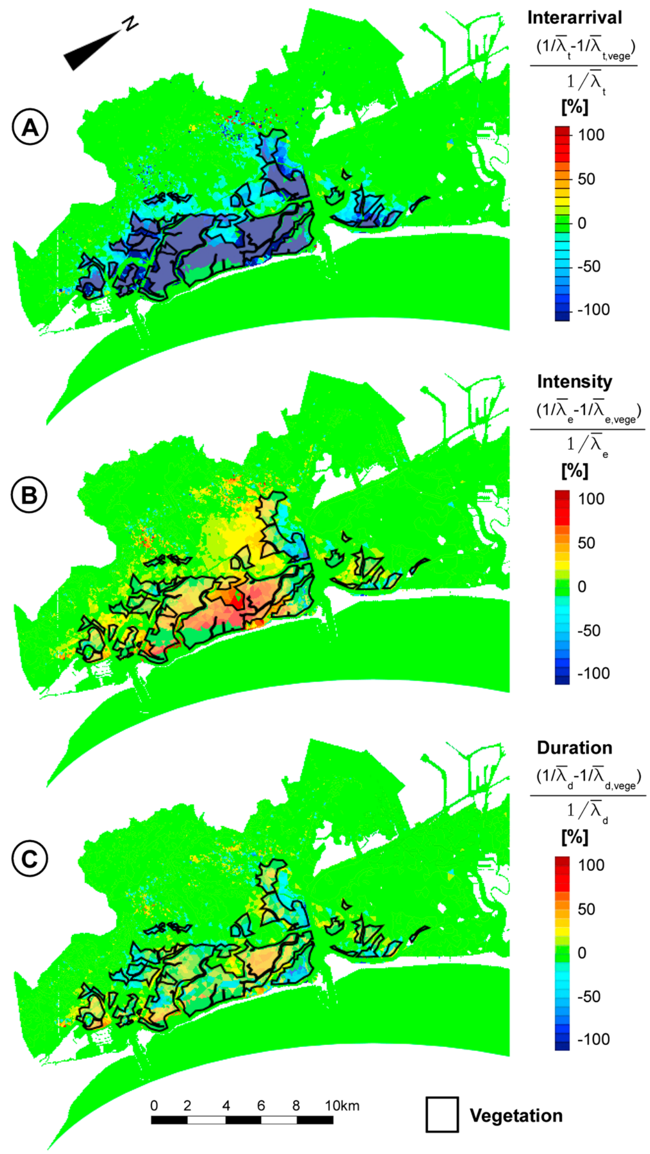

Figure 8. Map reproducing the planimetric distribution of the difference between (a) the mean interarrival times, (b) mean intensities of peak excesses, and (c) mean durations of over threshold exceedances obtained neglecting and considering the stabilizing effect of submerged benthic vegetation. Shaded areas bordered by black lines represent the extent of the sea grass meadows colonizing this portion of the lagoon (see Figure 2).

means (over the entire lagoon) of the statistical parameters computed in Table 1 shows that the most visible effect of sea grass meadows is to increase the spatially averaged mean interarrival time (from about 29 days without vegetation to 36 days with vegetation) and to slightly decrease the spatially averaged mean intensity (from about 73 mg/L to about 67 mg/L). Instead, the values obtained for the other statistics (including the coefficients of variation and the spatial cross correlations among interarrival time, intensity, and duration) are poorly affected by the presence of benthic vegetation.

We believe that the above results may help improving our understanding of suspended sediment dynamics in tidal environments. In particular, we speculate that our findings may be instrumental in improving our capability of evaluating the long-term morphodynamic evolution of shallow microtidal environments by properly accounting for the stochasticity of sediment supply driven by wind-induced resuspension events.

Modeling tidal-landscape morphodynamic evolution over long timescales (decades or centuries) necessarily requires the use of simplified approaches. Long-term evolution models usually assume sediment supply as constant or monotonically related to mean water depth. Analogously, the time sequence used to characterize erosion events is frequently oversimplified or neglected altogether (e.g., when considering vegetated salt marshes). Our results, combined with those obtained by *D'Alpaos et al.* [2013], demonstrate that the time series of both BSS and SSC can be described as marked Poisson processes with exponentially distributed interarrival times, intensities, and durations, thereby setting a framework for the synthetic generation of statistically significant external forcings (shear stress at the bottom and suspended sediment available in the water column) that should arguably improve the reliability of long-term biomorphodynamic models at the cost of a limited increase in the number of parameters. Within such a framework, one could also conceive to deal with ensemble averages of different realizations, which would allow one to obtain quantitative estimates of the uncertainty and the confidence intervals associated to long-term predictions. On this topic, research is ongoing.

4. Conclusions

Numerical models can overcome the intrinsic limitations of direct SSC observations (like those provided by probes or satellite images typically used for monitoring tidal environments). Once calibrated and tested, numerical models provide reliable, arbitrary long SSC time series which can be analyzed in order to statistically characterize the spatial and temporal dynamics of resuspension events by accounting in full for the geomorphological complexity of tidal environments. In the present study a calibrated and tested Wind Wave-Tidal Model coupled with a sediment transport model were used to perform a simulation reproducing a representative year for the wind characteristics in the Venice lagoon.

The computed SSC time series was analyzed on the basis of the Peak Over Threshold theory. Statistical analyses suggest that resuspension events can be modeled as a marked Poisson process over wide areas of the Venice lagoon both in terms of BSS (as demonstrated by *D'Alpaos et al.* [2013]) and in terms of SSC.

Our analysis on the SSC records shows that on average every month, the whole lagoon experiences wind-wave-driven resuspension events lasting about 14 h and characterized by an average peak value of SSC of about 70 mg/L. Furthermore, we observe that intensity of peak excesses and duration of over threshold exceedances are highly correlated, while almost no correlation exists between durations and interarrival times and between intensities and interarrival times. This suggests that resuspension events can be modeled as a 3-D marked Poisson process with marks (intensity and duration) mutually dependent but independent on the interarrival times.

The key role of advection/dispersion processes was observed based on the spatial patterns of mean interarrival times of SCC over threshold events that are notably less heterogeneous than the equivalent patterns obtained considering BSS over threshold events.

The biostabilizing effect of benthic vegetation that colonizes the central southern part of the Venice lagoon was also discussed based on the analysis of the modeled SSC records. The spatial distribution of the statistics of over threshold events, in cases when the stabilizing effect of sea grass meadows is selectively accounted for or neglected, suggests that the presence of wide areas colonized by benthic vegetation induces a local decrease in the frequency of significant resuspension events that tends to expand also to the surrounding regions. Sparse meadows have, instead, almost no effect on the SSC patterns because of the nonlocal nature of SSC dynamics. Compared to the effect of vegetation on the mean interarrival time, the impact on the other spatiotemporal patterns of SSCs (i.e., mean intensity and duration) is limited. Overall, our results suggest the crucial interaction between physical and biological processes in determining sediment dynamics in tidal environments and their biomorphological evolution.

The authors believe that the present findings bear significant implications for long-term morphodynamic models, as they provide a theoretical framework for generating statistically realistic synthetic forcings which can be used to predict the effect of biomorphodynamic processes on the fate of tidal landforms.

Acknowledgments
This research was supported by Comune di Venezia "Modificazioni morfologiche della laguna, perdita e reintroduzione dei sedimenti" by the 2013 University of Padova project "Combined use of remote sensing and in situ measurements for the calibration of transport and diffusion models in shallow coastal lagoons" (CPDA133253/13) and by the CARIPARO Project titled "Reading signatures of the past to predict the future: 1000 years of stratigraphic record as a key for the future of the Venice Lagoon". The data for this paper are available by contacting the corresponding author.

References

Amos, C. L., A. Bergamasco, G. Umgiesser, S. Cappucci, D. Cloutier, L. DeNat, M. Flindt, M. Bonardi, and S. Cristante (2004), The stability of tidal flats in Venice lagoon—The results of in-situ measurements using two benthic, annular flumes, *J. Mar. Syst.*, *51*, 211–241.

Balkema, A. A., and L. de Haan (1974), Residual life time at great age, *Ann. Probab.*, *2*, 792–804.

Botter, G., A. Porporato, I. Rodriguez-Iturbe, and A. Rinaldo (2007), Basin-scale soil moisture dynamics and the probabilistic characterization of carrier hydrologic flows: Slow, leaching-prone components of the hydrologic response, *Water Resour. Res.*, *43*, W02417, doi:10.1029/2006WR005043.

Botter, G., S. Basso, I. Rodriguez-Iturbe, and A. Rinaldo (2013), Resilience of river flow regimes, *Proc. Natl. Acad. Sci. U.S.A.*, *110*(32), 12,925–12,930, doi:10.1073/pnas.1311920110.

Breugem, W., and L. Holthuijsen (2006), Generalized shallow water wave growth from Lake George, *J. Waterw. Port Coastal Ocean Eng.*, *133*(3), 173–182, doi:10.1061/(ASCE)0733-950X(2007)133:3(173).

Callaghan, D. P., T. J. Bouma, P. Klaassen, D. van der Wal, M. J. F. Stive, and P. M. J. Herman (2010), Hydrodynamic forcing on salt-marsh development: Distinguishing the relative importance of waves and tidal flows, *Estuarine Coastal Shelf Sci.*, *89*, 73–88, doi:10.1016/j.ecss.2010.05.013.

Carniello, L., A. Defina, S. Fagherazzi, and L. D'Alpaos (2005), A combined Wind Wave-Tidal Model for the Venice lagoon, Italy, *J. Geophys. Res.*, *110*, F04007, doi:10.1029/2004JF000232.

Carniello, L., A. Defina, and L. D'Alpaos (2009), Morphological evolution of the Venice lagoon: Evidence from the past and trend for the future, *J. Geophys. Res.*, *114*, F04002, doi:10.1029/2008JF001157.

Carniello, L., A. D'Alpaos, and A. Defina (2011), Modeling wind-waves and tidal flows in shallow microtidal basins, *Estuarine Coastal Shelf Sci.*, *92*, 263–276, doi:10.1016/j.ecss. 2011.01.001.

Carniello, L., A. Defina, and L. D'Alpaos (2012), Modeling sand-mud transport induced by tidal currents and wind waves in shallow microtidal basins: Application to the Venice lagoon (Italy), *Estuarine Coastal Shelf Sci.*, *102–103*, 105–115, doi:10.1016/j.ecss.2012.03.016.

Carniello, L., S. Silvestri, M. Marani, A. D'Alpaos, V. Volpe, and A. Defina (2014), Sediment dynamics in shallow tidal basins: In situ observations, satellite retrievals, and numerical modeling in the Venice lagoon, *J. Geophys. Res. Earth Surface*, *119*, 802–815, doi:10.1002/2013JF003015.

Carr, J. A., P. D'Odorico, K. McGlathery, and P. Wiberg (2010), Stability and bistability of seagrass ecosystems in shallow coastal lagoons: Role of feedbacks with sediment resuspension and light attenuation, *J. Geophys. Res.*, *115*, G03011, doi:10.1029/2009JG001103.

Carr, J. A., P. D'Odorico, K. McGlathery, and P. Wiberg (2015), Spatially explicit feedbacks between seagrass meadow structure, sediment and light: Habitat suitability for seagrass growth, *Adv. Water Resour.*, doi:10.1016/j.advwatres.2015.09.001, in press.

Cramer, H., and M. R. Leadbetter (1967), *Stationary and Related Stochastic Processes*, John Wiley, 348 pp., New York.

Curiel, D., A. Rismondo, G. Bellemo, and M. Marzocchi (2004), Macroalgal biomass and species variations in the lagoon of Venice (North Adriatic Sea, Italy), *Sci. Mar.*, *68*(1), 57–67.

Da Lio, C., A. D'Alpaos, and M. Marani (2013), The secret gardener: Vegetation and the emergence of biogeomorphic patterns in tidal environments, *Philos. Trans. R. Soc. A*, *371*, 20120367, doi:10.1098/rsta.2012.0367.

D'Alpaos, A., and M. Marani (2015), Reading the signatures of biologic-geomorphic feedbacks in salt-marsh landscapes, *Adv. Water Resour.*, doi:10.1016/j.advwatres.2015.09.004, in press.

D'Alpaos, A., S. Lanzoni, M. Marani, and A. Rinaldo (2007a), Landscape evolution in tidal embayments: Modeling the interplay of erosion sedimentation and vegetation dynamics, *J. Geophys. Res.*, *110*, F01008, doi:10.1029/2006JF000537.

D'Alpaos, A., L. Carniello, and S. M. Mudd (2011), Dynamic response of marshes to perturbations in suspended sediment concentrations and rates of relative sea level rise, *J. Geophys. Res.*, *116*, F04020, doi:10.1029/2011JF002093.

D'Alpaos, A., L. Carniello, and A. Rinaldo (2013), Statistical mechanics of wind wave-induced erosion in shallow tidal basins: Inferences from the Venice lagoon, *Geophys. Res. Lett.*, *40*, 3402–3407, doi:10.1002/grl.50666.

D'Alpaos, L. (2010), *Fatti e Misfatti di Idraulica Lagunare*, Istituto Veneto di Scienze Lettere ed Arti, 329 pp., Venezia, Italy.

D'Alpaos, L., and A. Defina (2007), Mathematical modeling of tidal hydrodynamics in shallow lagoons: A review of open issues and applications to the Venice lagoon, *Comput. Geosci.*, *33*(4), 476–496, doi:10.1016/j.cageo.2006.07.009.

Defina, A. (2000), Two dimensional shallow flow equations for partially dry areas, *Water Resour. Res.*, *36*(11), 3251–3264.

Defina, A., L. Carniello, S. Fagherazzi, and L. D'Alpaos (2007), Self-organization of shallow basins in tidal flats and salt marshes, *J. Geophys. Res.*, *112*, F03001, doi:10.1029/2006JF000550.

D'Odorico, P., and S. Fagherazzi (2003), A probabilistic model of rainfall-triggered shallow landslides in hollows: A long-term analysis, *Water Resour. Res.*, *39*(9), 1262, doi:10.1029/2002WR001595.

Fagherazzi, S., L. Carniello, L. D'Alpaos, and A. Defina (2006), Critical bifurcation of shallow microtidal landforms in tidal flats and salt marshes, *Proc. Natl. Acad. Sci. U.S.A.*, *103*(22), 8337–8341, doi:10.1073/pnas.0508379103.

Folkard, A. M. (2005), Hydrodynamics of model Posidonia oceanica patches in shallow water, *Limnol. Oceanogr.*, *50*(5), 1592–1600, doi:10.4319/lo.2005.50.5.1592.

Gartner, J. W. (2004), Estimating suspended solids concentrations from backscatter intensity measured by acoustic doppler current profiler in San Francisco Bay, California, *Mar. Geol.*, *211*, 169–187, doi:10.1016/j.margeo.2004.07.001.

Grass, A. (1970), Tinitial instability of fine bed sand, *J. Hydraul. Div.*, *96*, 619–632.

Green, M. O., and G. Coco (2007), Sediment transport on an estuarine intertidal flat: Measurements and conceptual model of waves, rainfall and exchanges with a tidal creek, *Estuarine Coastal Shelf Sci.*, *72*, 553–569, doi:10.1016/j.ecss.2006.11.006.

Green, M. O., and G. Coco (2014), Review of wave-driven sediment resuspension and transport in estuaries, *Rev. Geophys.*, *52*, 77–117, doi:10.1002/2013RG000437.

Hendriks, I. E., T. J. Bouma, E. P. Morris, and C. M. Duarte (2010), Effects of seagrasses and algae of the Caulerpa family on hydrodynamics and particle-trapping rates, *Mar. Biol.*, *157*, 473–481, doi:10.1007/s00227-009-1333-8.

Hughes, Z. J., D. M. FitzGerald, C. A. Wilson, S. C. Pennings, K. Wi ski, and A. Mahadevan (2009), Rapid headward erosion of marsh creeks in response to relative sea level rise, *Geophys. Res. Lett.*, *36*, L03602, doi:10.1029/2008GL036000.

Kirwan, M., and B. Murray (2007), A coupled geomorphic and ecological model of tidal marsh evolution, *Proc. Natl. Acad. Sci. U.S.A.*, *104*(15), 6118–6122, doi:10.1073/pnas.0700958104.

Lawson, S. E., P. L. Wiberg, K. J. McGlathery, and D. C. Fugate (2007), Wind-driven sediment suspension controls light availability in a shallow coastal lagoon, *Estuaries Coasts*, *30*(1), 102–112, doi:10.1007/BF02782971.

Lopez, F., and M. H. Garcia (2001), Mean flow and turbulence structure of open-channel flow through non-emergent vegetation, *J. Hydraul. Eng.*, *127*(5), 392–402.

Marani, M., A. D'Alpaos, S. Lanzoni, L. Carniello, and A. Rinaldo (2007), Biologically-controlled multiple equilibria of tidal landforms and the fate of the Venice lagoon, *Geophys. Res. Lett.*, *34*, L11402, doi:10.1029/2007GL030178.

Marani, M., A. D'Alpaos, S. Lanzoni, L. Carniello, and A. Rinaldo (2010), The importance of being coupled: Stable states and catastrophic shifts in tidal biomorphodynamics, *J. Geophys. Res.*, *115*, F04004, doi:10.1029/2009JF001600.

Marani, M., C. Da Lio, and A. D'Alpaos (2013), Vegetation engineers marsh morphology through multiple competing stable states, *Proc. Natl. Acad. Sci. U.S.A.*, *110*(9), 3259–3263, doi:10.1073/pnas.1218327110.

Mariotti, G., and J. Carr (2014), Dual role of salt marsh retreat: Long-term loss and short-term resilience, *Water Resour. Res.*, *50*, 2963–2974, doi:10.1002/2013WR014676.

Mariotti, G., and S. Fagherazzi (2013), Critical width of tidal flats triggers marsh collapse in the absence of sea-level rise, *Proc. Natl. Acad. Sci. U.S.A.*, *110*(14), 5353–5356, doi:10.1073/pnas.1219600110.

Mariotti, G., S. Fagherazzi, P. Wiberg, K. McGlathery, L. Carniello, and A. Defina (2010), Influence of storm surges and sea level on shallow tidal basin erosive processes, *J. Geophys. Res.*, *115*, C11012, doi:10.1029/2009JC005892.

Martini, P., L. Carniello, and C. Avanzi (2004), Two dimensional modelling of flood flows and suspended sediment transport: The case of brenta river, Veneto (Italy), *Nat. Hazards Earth Syst. Sci.*, *4*(1), 165–181.

Molinaroli, E., S. Guerzoni, A. Sarretta, M. Masiol, and M. Pistolato (2009), Thirty-year changes (1970 to 2000) in bathymetry and sediment texture recorded in the lagoon of Venice sub-basins, Italy, *Mar. Geol.*, *258*, 115–125, doi:10.1016/j.margeo.2008.12.001.

Möller, I., T. Spencer, J. R. French, D. J. Leggett, and M. Dixon (1999), Wave transformation over salt marshes: A field and numerical modelling study from North Norfolk, England, *Estuarine Coastal Shelf Sci.*, *49*(3), 411–426, doi:10.1006/ecss.1999.0509.

Moore, K. A., and J. C. Jarvis (2008), Environmental factors affecting recent summertime eelgrass diebacks in the lower Chesapeake bay: Implications for long-term persistence, *J. Coastal Res.*, *55*, 135–147, doi:10.2112/SI55-014.

Morris, J. T., P. V. Sundareshwar, C. T. Nietch, B. Kjerfve, and D. R. Cahoon (2002), Responses of coastal wetlands to rising sea level, *Ecology*, *83*, 2869–2877, doi:10.1890/0012-9658(2002)083[2869:ROCWTR]2.0.CO;2.

Mudd, S. M., S. Howell, and J. T. Morris (2009), Impact of dynamic feedbacks between sedimentation, sea-level rise, and biomass production on near surface marsh stratigraphy and carbon accumulation, *Estuarine Coastal Mar. Sci.*, *82*, 377–389, doi:10.1016/j.ecss.2009.01.028.

Mudd, S. M., A. D'Alpaos, and J. T. Morris (2010), How does vegetation affect sedimentation on tidal marshes? Investigating particle capture and hydrodynamic controls on biologically mediated sedimentation, *J. Geophys. Res.*, *115*, F03029, doi:10.1029/2009JF001566.

Murray, A. B. (2007), Reducing model complexity for explanation and prediction, *Geomorphology*, *90*(3–4), 178–191, doi:10.1016/j.geomorph.2006.10.020.

Nepf, H. M., and E. R. Vivoni (2000), Flow structure in depth-limited, vegetated flow, *J. Geophys. Res.*, *105*(C12), 28,547–28,557, doi:10.1029/2000JC900145.

Neumeier, U., C. Ferrarin, C. L. Amos, G. Umgiesser, and M. Z. Li (2008), Sedtrans05: An improved sediment-transport model for continental shelves and coastal waters, *Comput. Geosci.*, *34*(10), 1223–1242.

Ouillon, S., P. Douillet, and S. Andréfouét (2004), Coupling satellite data with in situ measurements and numerical modeling to study fine suspended-sediment transport: A study for the lagoon of New Caledonia, *Coral Reefs*, *23*, 109–122, doi:10.1007/s00338-003-0352-z.

Park, J., G. Botter, J. Jawitz, and P. Rao (2014), Stochastic modeling of hydrologic variability of geographically isolated wetlands: Effects of hydro-climatic forcing and wetland bathymetry, *Adv. Water Resour.*, *69*, 38–48, doi:10.1016/j.advwatres.2014.03.007.

Perillo, G., D. Minkoff, and M. Piccolo (2005), Novel mechanism of stream formation in coastal wetlands by crab-fish-groundwater interaction, *Geo Mar. Lett.*, *25*, 214–220, doi:10.1007/s00367-005-0209-2.

Rodriguez-Iturbe, I., D. R. Cox, and V. Isham (1987), Some models for rainfall based on stochastic point processes, *Proc. R. Soc. A*, *410*, 269–288.

Ruhl, C. A., D. H. Schoellhamer, R. P. Stumpf, and C. L. Linds (2001), Combined use of remote sensing and continuous monitoring to analyse the variability of suspended-sediment concentrations in San Francisco Bay, *Estuarine Coastal Shelf Sci.*, *53*, 801–812, doi:10.1006/ecss.2000.0730.

SELC (2005), Attività di Monitoraggio Ambientale della Laguna di Venezia - MELa 2 - Carta della distribuzione delle fanerogame marine in Laguna di Venezia, *Tech. Rep.*, Magistrato alle Acque - Consorzio Venezia Nuova, Venezia, Italy.

Soulsby, R. L. (1997), *Dynamics of Marine Sands: A Manual for Practical Applications*, Thomas Telford, London.

Temmerman, S., G. Govers, P. Meire, and S. Wartel (2003), Modelling long-term tidal marsh growth under changing tidal conditions and suspended sediment concentrations, Scheldt estuary, Belgium, *Mar. Geol.*, *193*, 151–169, doi:10.1016/S0025-3227(02)00642-4.

Temmerman, S., T. J. Bouma, J. Van de Koppel, D. Van der Wal, M. B. De Vries, and P. M. J. Herman (2007), Vegetation causes channel erosion in a tidal landscape, *Geology*, *35*(7), 631–634, doi:10.1029/2004JF000243.

Van Ledden, M., Z. Wang, H. Winterwerp, and H. De Vriend (2004), Sand-mud morphodynamics in a short tidal basin, *Ocean Dyn.*, *54*, 385–391, doi:10.1007/s10236-003-0050-y.

Van Rijn, L. C. (1984), Sediment transport. Part II: Suspended load transport, *J. Hydraul. Eng.*, *110*(11), 1613–1641.

Venier, C., J. Figueiredo da Silva, S. J. McLelland, R. W. Duck, and S. Lanzoni (2012), Experimental investigation of the impact of macroalgal mats on flow dynamics and sediment stability in shallow tidal areas, *Estuarine Coastal Shelf Sci.*, *112*, 52–60, doi:10.1016/j.ecss.2011.12.

Venier, C., A. D'Alpaos, and M. Marani (2014), Evaluation of sediment properties using wind and turbidity observations in the shallow tidal areas of the Venice lagoon, *J. Geophys. Res. Earth Surf.*, *119*, 1604–1616, doi:10.1002/2013JF003019.

Volpe, V., S. Silvestri, and M. Marani (2011), Remote sensing retrieval of suspended sediment concentration in shallow waters, *Remote Sens. Environ.*, *115*, 44–54, doi:10.1016/j.rse.2010.07.013.

Wren, D. G., B. D. Barkdoll, R. A. Kuhnle, and R. W. Derrow (2000), Field techniques for suspended-sediment measurement, *J. Hydraul. Eng.*, *126*, 97–104.

Yang, Y. S., and L. Wang (2010), A review of modelling tools for implementation of the EU water framework directive in handling diffuse water pollution, *Water Resour. Manage.*, *24*(9), 1819–1843, doi:10.1007/s11269-009-9526-y.

Young, I., and L. Verhagen (1996), The growth of fetch-limited waves in water of finite depth. Part 1: Total energy and peak frequency, *Coastal Eng.*, *29*(1–2), 47–78.